Characterization of Three-Dimensional Tissue Cultures Using Electrical Impedance Spectroscopy

Alastair H. Kyle, Carmel T. O. Chan, and Andrew I. Minchinton
Department of Medical Biophysics, British Columbia Cancer Research Centre, Vancouver, British Columbia, Canada

ABSTRACT Electrical impedance spectroscopy was used to characterize the cell environment of multilayered cell cultures (MCCs), a culture system in which cells are grown on a permeable support membrane to form a thick disc of cells with tumor-like properties. Cultures were grown using SiHa tumor cells as well as V79 wild-type cells and V79/DOX cells cultivated to exhibit multidrug resistance. Electrical impedance measurements were made on MCCs over a frequency range of 0.1 kHz to 1 MHz. Data analysis using a simple electrical model for the cell environment yielded estimates for parameters related to the intra- and extracellular resistance and net membrane capacitance, which were then related to MCC thickness. The extracellular fraction and tortuosity of the MCCs were determined in separate experiments where the rate of diffusion and the equilibrium level of C^{14}-inulin, which does not penetrate the cell membrane, was measured within MCCs. Impedance measurements predicted the barrier to diffusion posed by the extracellular space of MCCs to be roughly two times greater than that inferred from the C^{14}-inulin experiments. However, the relative ranking of the three cell types used to grow MCCs was similar for the two methods. Results indicate that impedance spectroscopy is well suited for use in characterizing the MCC cell environment, offering a fast, nondestructive method for monitoring cell culture growth and integrity.

INTRODUCTION

Over the past 20 years, three-dimensional tissue cultures have been increasingly used to model the extravascular compartment of solid tumors. Usually, three-dimensional cultures have been grown in the form of spheroids (Durand and Olive, 1992; Mueller-Klieser, 1997; Sutherland, 1988) but recently cellular aggregates grown on permeable membranes to form multilayered cell cultures (MCCs) have been developed (Cowan et al., 1996; Minchinton et al., 1997). Spheroidal and multilayered cultures mimic the tumor environment better than monolayer cell cultures because their three-dimensional structure permits increased cell-to-cell interaction. Numerous studies examining differential effects of drugs and radiation on cell survival between monolayer and three-dimensional cultures have been reported (Durand, 1981; Kerr et al., 1987; Kwok and Sutherland, 1991; Olive and Durand, 1994). In addition, the barrier imposed by tumor tissue to penetration by therapeutic drugs has been examined using these models (Casciari et al., 1988; Hicks et al., 1997; Kerr and Kaye, 1987; Kyle and Minchinton, 1999; Nederman et al., 1981). MCCs are particularly well suited for use in studying drug flux and metabolism in tumor-like tissue because they are grown on permeable membranes that can be oriented to separate two reservoirs of a diffusion apparatus.

An obstacle to the interpretation and analysis of data obtained from diffusion experiments is the lack of methodology for characterizing the structure of individual MCCs or for determining variations between different cell lines grown as MCCs. Accurate assessment of culture thickness before experiments and the rate of growth during experiments, as well as knowledge of the fraction of extracellular space available for diffusion and the effect of drug toxicity on cultures, are all key factors in interpreting experimental data. Commonly, culture thickness is evaluated through either visual measurement of cryostat sections taken after experiments or diffusion of a molecule with a known diffusion coefficient for the specific MCCs (Cowan et al., 1996; Kyle and Minchinton, 1999). Both methods have drawbacks. Cryostat sectioning is time-consuming and it is difficult to obtain an accurate measure of average thickness of the culture. Cryostat sectioning also precludes the use of the culture for other experimental endpoints such as cell survival or accumulated drug content. Determination of culture thickness through flux measurement of a molecule with a known diffusion coefficient allows for good assessment of the effective culture thickness. However, this method generally involves carrying out a diffusion experiment over a few hours and, when done in conjunction with the diffusion of the therapeutic drug of interest, results may be skewed by changes to the cell culture environment which pass undetected. In addition to knowledge of culture thickness, the interpretation of results from drug flux experiments through MCCs also requires assessment of the extracellular space available to a drug for diffusion. Studies have been carried out to determine extracellular space in spheroids using equilibrium levels of molecules which do not pass the cell membrane and by cell volume measurements (Durand, 1980; Freyer and Sutherland, 1983). Results suggest the existence of large variations in extracellular space between tumor cell lines, with values ranging from 15 to 60%. Because the extracellular space may be the primary route of penetration into tumor tissue for many therapeutic

Received for publication 9 November 1998 and in final form 2 February 1999.

Address reprint requests to Dr. Andrew I. Minchinton, BC Cancer Research Centre, 601 West 10th Avenue, Vancouver BC V5Z 1L3, Canada. Tel.: 604-877-6182; Fax: 604-877-6002; E-mail: minc@unixg.ubc.ca.

0006-3495/99/05/2640/09 $2.00

drugs, it is critical that this factor be well characterized for any in vitro tumor model.

Although it is not practical with spheroids, the MCC geometry presents an opportunity for the application of electrical impedance spectroscopy (EIS) to study the cell environment of three-dimensional tissue cultures. EIS utilizes the inherent electrical properties of individual cells to quantitate macroscopic parameters related to the tissue environment (Cole and Cole, 1941; Foster and Schwan, 1989; Schwan, 1963). On a conceptual level, the cell cytoplasm and extracellular space act as conductive media isolated from each other by the cell membrane (Fig. 1 *a*). A simple electrical circuit (Fig. 1 *b*) can be constructed to represent these terms; where the conductivity of the extracellular space and cell cytoplasm contribute the resistive components, R_e and R_i (due largely to the presence of salt ions), and the cell membrane contributes the capacitive effect, C_m. Determining experimental values for these parameters allows for empirical comparison of impedance data with physical traits such as MCC thickness. Impedance results can also be used to estimate the relative barrier to diffusion posed by MCCs grown using different types of cells. This study investigates the ability of EIS to monitor the cell environment of MCCs grown using SiHa, V79, and V79/DOX (exhibiting multidrug resistance) cells.

THEORY

Impedance spectroscopy involves passing an alternating current over a range of frequencies through an object to determine the functional form of its electrical impedance. The application of this technique to biological material has been described by numerous investigators (Ackmann, 1993; Bao et al., 1993; McRae et al., 1997). The basic premise of the four-terminal system used by us and others is illustrated in Fig. 2 *a* and the schematic of a commercially available jig we used for these experiments is shown in Fig. 2 *b* (EndOhm-12). Two large-area stainless steel electrodes are used to pass a sine wave current of known amplitude and frequency through the material under study. The voltage drop and phase shift generated by the material is then measured by two small-area chloridized silver electrodes. How the voltage drop and phase shift vary with frequency is

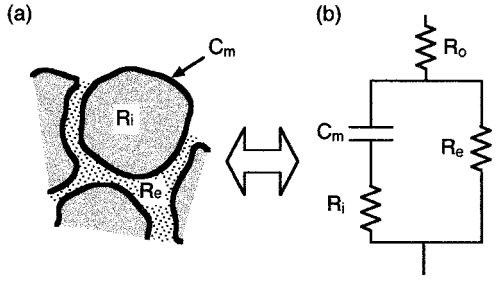

FIGURE 1 Illustration of a simplified cell environment (*a*) and the equivalent electrical circuit (*b*) that models the key parameters of intra- and extracellular conduction, R_i and R_e, and membrane capacitance, C_m.

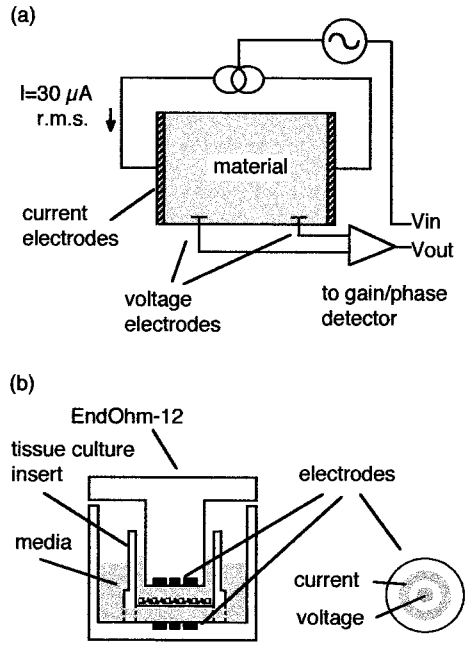

FIGURE 2 (*a*) Schematic of a typical four-electrode impedance measurement setup for biological material. Current is passed through two large-area electrodes by a constant current source driven by a sine wave generator. The voltage drop across the material is detected by two smaller electrodes connected to a high impedance differential amplifier that leads to a gain/phase detection system. (*b*) Diagram of the EndOhm-12, four-electrode measurement cell used for the experiments.

used to determine the functional form of the magnitude, Z, and phase, ϕ, of impedance of the culture. Where an arbitrary impedance can be written in the form

$$Z = A + iB, \tag{1}$$

with

$$|Z|^2 = A^2 + B^2 \tag{2}$$

and

$$\phi = \arctan(B/A), \tag{3}$$

here A and B are the real and imaginary components of the impedance and $i = (-1)^{1/2}$.

Modeling MCCs

The electrical properties of conduction and capacitance of the tumor cells are modeled empirically using a variation of Cole-Cole relaxation equation (Foster and Schwan, 1989) in which the membrane capacitive term is replaced with a constant phase element (CPE) term:

$$Z_{cell} = R_i + \frac{1}{(i\omega Y_o)^n} \tag{4}$$

where R_i is the net intracellular resistance, Y_o and n are the CPE terms that model membrane capacitance, ω is the angular frequency (defined as $\omega = 2\pi f$), and $i^n = \cos(n\pi/2) +$

$i \sin(n\pi/2)$. The CPE term is thought to better model the existence of a distribution of relaxation times often seen in biological material (for a recent review see Rigaud et al., 1996). When n is set to 1, the second term in Eq. 4 describes a purely capacitive effect. Generally, for biological tissue, n is found to be between 0.5 and 0.8 (Foster and Schwan, 1989).

The total impedance for the MCC can then be written as a combination of Z_{cell} and net extracellular resistance, R_e:

$$Z_{MCC} = \left(\frac{1}{R_e} + \frac{1}{Z_{cell}}\right)^{-1} = \frac{R_e[R_i(i\omega Y_o)^n + 1]}{(R_e + R_i)(i\omega Y_o)^n + 1}. \quad (5)$$

This relation can be expanded and then written in the form of Eq. 1 such that A and B are equated to functions of R_e, R_i, Y_o, n, and ω. Experimental estimates of the parameters R_e, R_i, Y_o, and n can then be determined, using Eqs. 2 and 3, through measurement of the voltage drop and phase shift generated by the MCC over a range of frequencies.

Estimating tissue tortuosity and the fraction of extracellular space in MCCs

If the conductivity of the growth media and the culture thickness are known, then an estimate of the combined effect of extracellular space and tissue tortuosity can be obtained through measurement of R_e. In general, the resistance of a cylindrical piece of purely conductive material can be written as:

$$R = \frac{\ell}{A} \cdot \frac{1}{\sigma} \quad (6)$$

where ℓ is the thickness, A is the surface area, and σ is the conductivity of the material. Applying this to the low-frequency impedance of an MCC, where the cell membrane acts as an insulator and one is effectively measuring the resistance of the extracellular space, yields the relation:

$$R_e = \frac{\ell'}{A'} \cdot \frac{1}{\sigma_e} \quad (7)$$

where σ_e is the conductivity of the extracellular medium and ℓ' and A' are the effective path length and cross-sectional area of the extracellular space. Taking ℓ' as equal to $\ell \cdot \lambda$, where λ is the tortuosity factor (Nicholson and Phillips, 1981) leads to A' being equal to $f \cdot V_T/(\ell \cdot \lambda) = f \cdot A/\lambda$. Here f is the fraction of extracellular space which is defined as $f = V_e/V_T$, where V_e and V_T are the volumes of the extracellular space and total MCC space, respectively. Substituting these results into Eq. 7 leads to the following relation:

$$R_e = \frac{\ell \cdot \lambda^2}{A \cdot f} \cdot \frac{1}{\sigma_e} \quad (8)$$

Measurement of R_e and ℓ and knowledge of A and σ_e then allows an estimate of the combined effect of tortuosity and fraction of extracellular space to be made. Rearranging Eq. 8 and defining φ as the ratio of f/λ^2, the factor by which tortuosity and extracellular space will modify measurement of R_e, leads to:

$$\varphi_{EIS} = \frac{\ell}{A} \cdot \frac{1}{R_e} \cdot \frac{1}{\sigma_e} \quad (9)$$

In a similar fashion, the effect of tissue tortuosity and the fraction of extracellular space on the diffusion of small molecules through the extracellular space of MCCs can be described using Fick's relation (Crank, 1975) for the steady state flux of a molecule through a slice of tissue of thickness ℓ and cross-sectional area A due to a concentration gradient ΔC:

$$\text{Flux} = DA \frac{\Delta C}{\ell} \quad (10)$$

where D is the diffusion coefficient of the molecule within the tissue.

If the molecule is constrained to the extracellular space then A and ℓ can be substituted for with A' and ℓ', as was done for Eq. 7, which leads to the following relation, consistent with the literature (Nicholson and Phillips, 1981):

$$\text{Flux} = D_w A' \frac{\Delta C}{\ell'} = \frac{f}{\lambda^2} D_w A \frac{\Delta C}{\ell} = \varphi_{diff} D_w A \frac{\Delta C}{\ell} \quad (11)$$

where D_w is the diffusion coefficient of the molecule in water and φ_{diff} is the diffusion analogue of the impedance parameter, φ_{EIS}. The parameter φ_{diff} will vary between cell lines and serves as a relative measure of the barrier presented by MCCs to the passage of a molecule which is constrained to diffuse through the extracellular space.

MATERIALS AND METHODS

Cells

SiHa (human cervix squamous cell carcinoma) cells were purchased from American Type Culture Collection (Manassas, VA). Chinese hamster V79–171b and V79/DOX cell lines were obtained from Dr. Ralph Durand (British Columbia Cancer Research Centre, Vancouver, BC). Cells were grown as monolayers using minimum essential media (10437–028, Gibco BRL, Burlington, ON) supplemented with 10% fetal bovine serum (15140–122, Gibco BRL) and passaged every 3 to 5 days upon reaching confluence. On every fourth passage, the V79/DOX cells were exposed to 5 μg/ml doxorubicin (Faulding, Vaudreuil, PQ) in order to maintain their drug resistance.

MCCs

The surface of the tissue culture plastic membrane (Millipore, Nepean, ON, CM 12 mm, pore size 0.4 μm, surface area 0.64 cm^2) was coated with 100 μl of a 0.75 mg/ml collagen (type I, Sigma Chemical, St. Louis, MO) solution (60% ethanol with 1.5 mM HCl) and allowed to dry overnight. Approximately 4×10^5 cells in 0.5 ml of growth media were then inoculated onto the coated surface of the membrane and incubated for 6–12 h to allow the cells to attach. Silicone o-rings placed around the inserts were used to support them in a frame with slots for six inserts. The frame was then completely immersed in 120 ml of stirred media. Cultures were incubated for up to 8 days with continual gassing (5% O_2, 5% CO_2, 90%

N_2) at 37.5°C. Media were changed daily after the first 3 days. Care was taken to avoid using MCCs that were not uniform over their entire surface area or that were thick enough to contain a necrotic middle region. In the range of MCC thicknesses used in these experiments, 0–250 μm, none of the MCCs exhibited a necrotic region.

Impedance measurement

Impedance measurements were made using the EndOhm-12 impedance cell (World Precision Instruments, Sarasota, FL) and a stripped-down version of an impedance measurement system described by Ackmann (1993), the basic premise of which is illustrated in Fig. 2 *a*. Briefly, a sine wave generator (Hewlett Packard 3312A) is used to drive a 30-μA r.m.s. current source (Ackmann, 1993) connected to one pair of the electrodes in the measurement cell. Voltage and phase measurements were then made using a buffered differential amplifier (d.c. gain = 9.18) connected to the second pair of electrodes and leading to an oscilloscope (Hitachi V-1085). For a given frequency, measurement of the voltage drop, V, across the culture yields $Z = V/I$ where I is fixed. The phase shift produced by the culture was then determined through comparison of V_{in} versus V_{out} using the oscilloscope in the X-Y mode. Measurements were carried out at room temperature over frequencies from 0.1 kHz to 1 MHz and took approximately 10 min per culture.

Calibration

A first-order calibration of the measurement system was made by determining the gain of the system as a function of frequency over the range of 0.1 kHz to 1 MHz. Fig. 3 shows results of measurements of gain made using the EndOhm-12 impedance cell with media and a tissue culture insert without cells. Data were fitted empirically using the function:

$$\text{gain}(f) = a \cdot e^{-f/\tau} + b \cdot f + a_o, \qquad (12)$$

where $a = 0.30$, $a_o = 8.9$, $b = 4.1 \times 10^{-4}$ kHz^{-1}, $\tau = 11$ kHz, and f is the measurement frequency in kHz. The magnitude of the impedance for subsequent measurements of V at a given frequency was calculated using the relation $Z = V/I \times 1/\text{gain}$, where I was fixed at 30 μA r.m.s.

Phase shifts were observed from measurement of purely resistive media alone, also shown in Fig. 3. Data were fitted using a linear relation between phase shift, ϕ, and frequency, f. Fitting the data to $\phi = 2\pi f \Delta t$ resulted in $\Delta t = (8.2 \pm 0.2) \times 10^{-8}$ s. This effect was then subtracted from subsequent phase measurements on cultures.

Cell factor

The measured resistance for an electrically conductive medium is related to its conductivity by Eq. 6, where ℓ is taken as the distance between the voltage-measuring electrodes, A is the cross-sectional area of the measurement cell, and σ is the conductivity of the medium. In practice, the cell factor, defined as ℓ/A, is determined experimentally using a medium of known conductivity. Using a 150-mM saline solution ($\sigma = 1.83$ S/m) (Pethig, 1979) we obtained a resistivity of $16.7 \pm 0.4\ \Omega$, which leads to a cell factor of 0.30 ± 0.01 cm^{-1}. This result compares favorably with an approximate value for the cell factor of 0.35 cm^{-1} obtained using $\ell = 0.275$ cm and $A \approx 0.79$ cm^2. Using the above result we determined the conductivity of our growth media to be 1.95 ± 0.05 S/m.

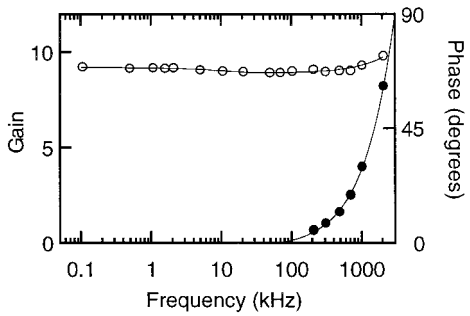

FIGURE 3 Calibration of our measurement system. Plot of gain (○) and phase shift (●) measured across a purely conductive medium. Lines show results of fitting the data as a function of frequency. Results were used in the analysis of subsequent impedance measurements.

Determination of MCC thickness

MCCs used for impedance measurements ranged from 80 to 250 μm thick. The thickness of each MCC was determined by its permeability to tritiated water using diffusion experiments described elsewhere (Kyle and Minchinton, 1999). Generally, impedance measurements were carried out first and were followed by a 2- to 4-h tritiated water experiment. Use of tritiated water allowed for a more reliable measurement of culture thickness than cryostat sectioning. Briefly, tritiated water was determined to exhibit a constant diffusion coefficient in each of the cell lines, with experimental values for D of $D_{SiHa} = (3.5 \pm 0.1) \times 10^{-6}$ cm^2/s, $D_{V79} = (2.9 \pm 0.1) \times 10^{-6}$ cm^2/s and $D_{V79/DOX} = (2.2 \pm 0.1) \times 10^{-6}$ cm^2/s. Culture thickness, ℓ, was then calculated using $\ell = D/P$, where P is the permeability determined experimentally for each culture. This method allowed for the determination of a weighted average of the culture thickness over its entire surface area.

Measurement of the fraction of extracellular space

Equilibrium levels of radiolabeled inulin (C^{14}-inulin, Amersham Life Science, Oakville, ON) within MCCs were used to determine the extracellular water fraction. MCCs of known thickness (determined via permeability to tritiated water) were incubated with 0.2 μCi/ml C^{14}-inulin for 4 h under controlled gassing, stirring, and temperature conditions to allow equilibration of C^{14}-inulin throughout the extracellular space of the cultures. After incubation, the cultures were quickly rinsed in fresh media for 10 s and then carefully wicked with a tissue to remove excess liquid from the surface of the culture. Each culture was then placed in a 20-ml scintillation vial with 500 μl of tissue solubilizing agent, Scintigest (Fisher Scientific, Nepean, ON), and left for 1 h. Following dissolution of the tissue, 10 ml of scintillation liquid, Scintisafe Econo-1 (Fisher Scientific) was added to each vial, which was then vigorously shaken for 1 min. Vials were left in darkness for 1 h and disintegrations then measured using a RackBeta scintillation counter (Turku, Finland). Scintillation decays per minute from the MCCs were compared with decays per minute from 100-μl samples of the original incubation medium containing the C^{14}-inulin to calculate the volume of space occupied by the C^{14}-inulin within the MCCs. The effect of the C^{14}-inulin contained within the permeable plastic was determined by separate experiments using inserts with no cells. This effect was then subtracted from the results of experiments done with cells, correcting the apparent fraction of extracellular space by a value <0.05.

Measurement of the rate of diffusion of C^{14}-inulin through MCCs

Flux data for C^{14}-inulin through MCCs were obtained from diffusion experiments similar to those for tritiated water. Typically, diffusion experiments were carried out over 2–4 h, with 0.07 μCi/ml C^{14}-inulin initially added to the donating side of a dual reservoir diffusion apparatus. Flux data were then analyzed assuming Fickean diffusion through the extracellular space, i.e., that flux of a molecule is proportional to concentration gradient across a section of tissue. The partial differential equation form of Fick's law, relating flux through infinitesimal slices of tissue, can be written

(Crank, 1975) as:

$$\frac{\partial c}{\partial t} = D\frac{\partial^2 c}{\partial x^2} \tag{13}$$

where D (cm^2/s) is the effective diffusion coefficient of C^{14}-inulin in the extracellular space of the MCC and c (mol/l) is the concentration of C^{14}-inulin, a function of both time, t, and position, x, within the MCC. D can be related to the diffusion coefficient of C^{14}-inulin in water, D_w, through the relation $D = D_w/\lambda^2$, where λ is the tortuosity factor (Nicholson and Phillips, 1981).

The boundary condition relating molecule flux from the donating reservoir into the extracellular space of the MCC was taken as (Crank, 1975):

$$V\frac{dC_1}{dt} = f \cdot A \cdot D\left.\frac{\partial c}{\partial x}\right|_{\text{reservoir1}} \tag{14}$$

where V is the reservoir volume, C_1 is the concentration of C^{14}-inulin in the donating reservoir, f is the fraction of extracellular space, and A is the MCC cross-sectional area.

The boundary condition for the interface between the MCC and the permeable plastic membrane, which equates the flux from one material to the flux into the other, was taken as (Crank, 1975):

$$\text{Flux} = f \cdot A \cdot D\left.\frac{\partial c}{\partial x}\right|_{\text{MCC side}} = A \cdot D'\left.\frac{\partial c}{\partial x}\right|_{\text{insert side}} \tag{15}$$

where Flux (mol/s) is the flux of C^{14}-inulin from one material to the other and D′ is the diffusion coefficient of C^{14}-inulin in the permeable plastic membrane.

The diffusion coefficient of C^{14}-inulin within the permeable plastic membrane, D′, was determined through diffusion experiments carried out using inserts with no cells attached. Using this approach, the effect of unstirred boundary layers located on either side of the insert were incorporated into an effective diffusion coefficient for the plastic membrane. The effects of the unstirred boundary layers and the plastic membrane were then described as a single layer 30 μm thick with diffusion coefficient D′, determined as 6.4×10^{-7} cm^2/s.

The boundary condition relating molecule flux from the plastic membrane into the receiving reservoir is similar to Eq. 11 but with a negative sign to account for the change of direction of flux, which will produce a positive increase in the reservoir concentration:

$$V\frac{dC_2}{dt} = -A \cdot D'\left.\frac{\partial c}{\partial x}\right|_{\text{reservoir2}} \tag{16}$$

where C_2 is the C^{14}-inulin concentration in the receiving reservoir.

Eqs. 10–13 were discretized using the implicit Crank-Nicolson method (Crank, 1975) and solved numerically on a Power Macintosh using the C programming language. Spatial step sizes were kept to 5 μm and temporal steps to 15 s. Drug flux data were then fitted to the model using the Levenberg-Marquardt nonlinear, χ-squared minimization technique (Press, 1992) to determine experimental estimates for the diffusion coefficient of C^{14}-inulin within the MCCs.

RESULTS

Typical data from electrical impedance measurements using a 3-day-old V79 MCC are shown in Fig. 4. The data were fitted using the impedance model described by Eq. 5, with an additional series term, R_o, to account for the resistance contributed by the growth medium. Impedance magnitude and phase data were fitted simultaneously using the Levenberg-Marquardt nonlinear, χ-squared minimization technique (Press, 1992). Model parameters were determined as

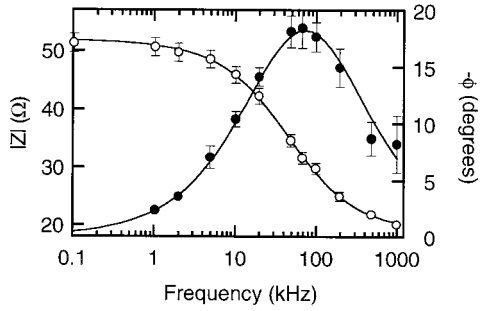

FIGURE 4 Typical results from measurement of impedance magnitude and phase as a function of frequency (Z - ○, ϕ - ●) on a 3-day-old, 145-μm-thick V79 MCC. Both data sets were fitted simultaneously to Eq. 5 to determine estimates of the parameters R_e, R_i, Y_o, and n.

$R_e = 34.4 \pm 0.8\ \Omega$, $R_i = 1.6 \pm 0.8\ \Omega$, $Y_o = (3.3 \pm 0.8) \times 10^{-8}$, and $n = 0.73 \pm 0.03$, with $R_o = 17.5\ \Omega$. Standard errors for model parameters calculated by the fitting routine were based on a predetermined measurement error of 3%. Use of tritiated water determined the culture to be 145 ± 5 μm thick.

Fig. 5 shows results for estimates of model parameters R_e, R_i, Y_o, and n as a function of culture thickness from a series of experiments using SiHa MCCs. The parameter representing extracellular resistance, R_e (Fig. 5 *a*), shows a curved increase with MCC thickness. If the structure of the MCC extracellular space remained unchanged with increasing MCC thickness, then the parameter R_e would be expected to increase linearly with MCC thickness. In this case, the curved relation of R_e to thickness suggests an increase to the barrier posed by the MCC, via either increased tortuosity or decreased fraction of extracellular space, with increasing MCC thickness. Data for R_e fitted using a second order polynomial, with the constant term forced to zero to match the physical situation of zero impedance for an MCC of zero thickness, yielded a linear term of $0.14 \pm 0.01\ \Omega/\mu$m and a quadratic term of $(9.5 \pm 0.5) \times 10^{-4}\ \Omega/\mu m^2$. Determination of R_i, the cytoplasm resistance (Fig. 5 *b*), was more difficult due to its small value relative to the system measurement error. It shows an upward trend, as expected, with increased culture thickness. Data for R_i fitted using a linear relation, with the constant term forced to zero, yielded a slope of $0.024 \pm 0.001\ \Omega/\mu$m. The parameter Y_o (Fig. 5 *c*), which models the membrane capacitance effect, shows a downward trend, consistent with the expected decrease in net MCC capacitance with an increase in the number of cell layers. Data for Y_0 fitted using second-order polynomial yielded the following fitting terms: constant term $(3.7 \pm 0.04) \times 10^{-7}$, linear term of $(-2.8 \pm 0.5) \times 10^{-9}\ \mu m^{-1}$, and quadratic term of $(5.9 \pm 1.4) \times 10^{-12}\ \mu m^{-2}$. The parameter n (Fig. 5 *d*) also decreases with increasing thickness. When fitted to a linear relation, a constant term of 0.91 ± 0.03 and a linear term of $(-2 \pm 1) \times 10^{-4}\ \mu m^{-1}$ were obtained.

Fig. 6 shows R_e, Y_o, and n plotted as a function of thickness, as obtained from a series of experiments using

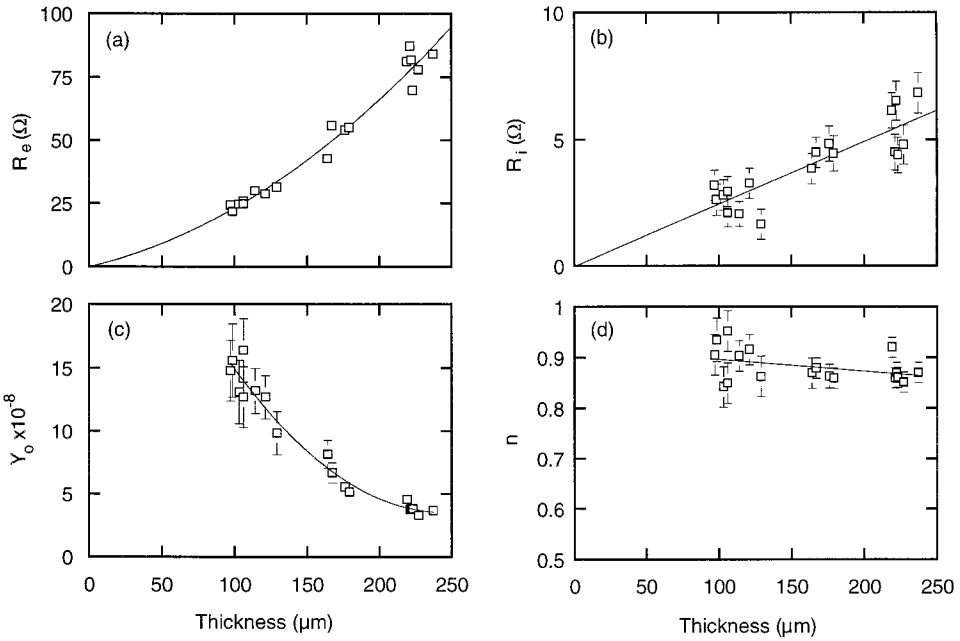

FIGURE 5 Results of impedance measurements from a series of experiments using MCCs grown with SiHa cells: (*a*) R_e, (*b*) R_i, (*c*) Y_o, and (*d*) n. Each data set was fit empirically as a function of culture thickness.

MCCs comprised of V79 and V79/DOX cells. In comparison with Fig. 5 *a*, the SiHa and V79 MCCs yielded similar R_e values. However, the V79/DOX MCCs produced higher R_e values at each thickness. The data for R_e from the V79 cells was fitted using a second-order polynomial with the constant term forced to zero, yielding a linear term of $0.15 \pm 0.01\ \Omega/\mu m$ and a quadratic term of $(5.9 \pm 1) \times 10^{-4}\ \Omega/\mu m^2$. The V79/DOX data for R_e could be fitted to a simple linear relation and still satisfy the requirement of zero impedance at zero thickness; a slope of $0.35 \pm 0.01\ \Omega/\mu m$ was obtained from the fit. Results for the parameter R_i for the V79 and V79/DOX MCCs are not shown because the measurement error, $\sim 1\ \Omega$, was generally as large as the values themselves. R_i ranged from 0 to 2Ω for the V79 MCCs and from 0 to $1\ \Omega$ for the V79/DOX MCCs. The difference in Y_o and n between the two cell types (Fig. 6, *b* and *c*), may be related to differences in cell density caused by differences in the extracellular fraction or average cell volume, which would affect the total membrane capacitance of an MCC. The differences between the SiHa, V79, and V79/DOX MCCs indicate that it is possible to differentiate between cell types grown to form MCCs using their impedance characteristics.

Fig. 7 shows an estimation of the fraction of extracellular space made via the measurement of equilibrium levels of C^{14}-inulin within SiHa, V79, and V79/DOX MCCs. The results indicate a general trend of extracellular space decreasing with MCC thickness, with the exception of the SiHa MCCs, in which this was not detected. These results are similar in magnitude to those reported in the literature for V79 spheroid cultures (Durand, 1980; Freyer and Sutherland, 1983). Fitting the results as a linear function of MCC thickness yielded constant terms of 0.22, 0.50, and 0.39 and slopes of $0.2 \times 10^{-4}\ \mu m^{-1}$, $-8.2 \times 10^{-4}\ \mu m^{-1}$, and $-7.1 \times 10^{-4}\ \mu m^{-1}$ for SiHa, V79, and V79/DOX MCCs, respectively.

Fig. 8 shows experimental estimates of the tortuosity factor, λ, within the extracellular spaces of SiHa, V79, and V79/DOX MCCs as determined from a series of flux experiments using C^{14}-inulin. Data from each flux experiment were analyzed according to Eqs. 13–16 to determine the apparent rate of diffusion, D, of C^{14}-inulin within the extracellular space of the MCC. λ was then estimated using $\lambda^2 = D_w/D$, where D_w is the rate of diffusion of C^{14}-inulin in water. The value of D_w for C^{14}-inulin was taken as approximately $3 \times 10^{-6}\ cm^2/s$ (Jain, 1987). Despite having accounted for the different extracellular fractions of the three cell types, there were still large variations among the three cell lines in the estimate of λ. These differences can be attributed to a variety of factors including cell size ($\sim 800\ \mu m^3$ for V79 cells (Freyer et al., 1984) versus $\sim 1800\ \mu m^3$ for SiHa cells), as well as differences in the composition of the extracellular space and cell-cell interactions. Fitting the results as a linear function of MCC thickness yielded constant terms of 1.75, 1.55, and 2.66 and slopes of $0.4 \times 10^{-3}\ \mu m^{-1}$, $7.4 \times 10^{-3}\ \mu m^{-1}$, and $3.0 \times 10^{-3}\ \mu m^{-1}$ for SiHa, V79, and V79/DOX cells, respectively.

Fig. 9 shows a comparison of the combined effect of tissue tortuosity and the extracellular fraction made from the impedance measurements and from the rate of diffusion of C^{14}-inulin within the extracellular space of MCCs. The φ term in Eqs. 9 and 11 describes how tortuosity and the fraction of extracellular space combine to determine the barrier posed by the MCCs to the flux of molecules. Fig. 9 *a* shows results from calculation of φ_{EIS} using Eq. 9 and the impedance data shown in Figs. 5 *a* and 6 *a*. Fig. 9 *b* shows similar results for calculation of φ_{Inulin} using Eq. 11 and the results for diffusion of C^{14}-inulin shown in Fig. 8. The

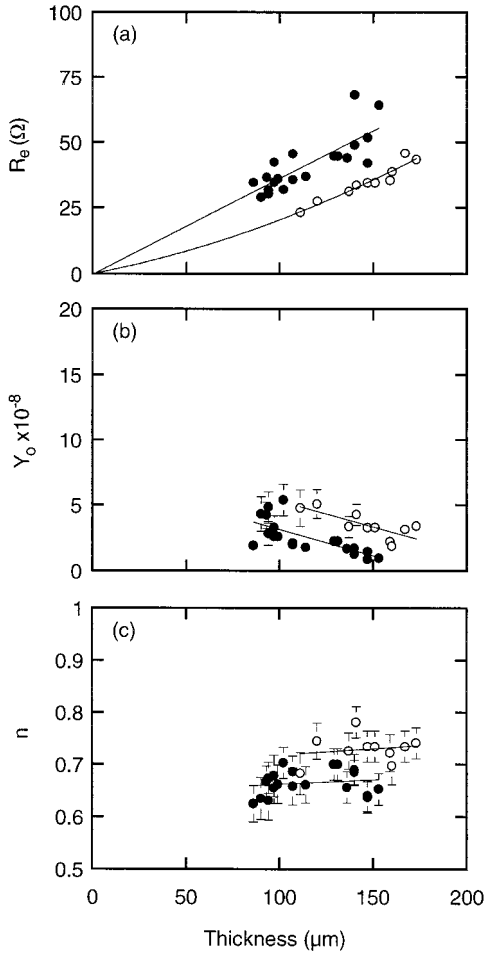

FIGURE 6 Results of impedance measurements from a series of experiments using MCCs grown with V79 ○ and V79/DOX ● cells: (*a*) R_e, (*b*) Y_o, and (*c*) n. Each data set was fit empirically as a function of culture thickness.

results of the two graphs indicate the extent to which impedance measurements can predict the effect of the MCC environment on C^{14}-inulin flux. The values for φ_{EIS} and φ_{Inulin} differ by roughly a factor of two. In both cases, SiHa and V79 MCCs are observed to rank higher than V79/DOX MCCs; however, the trends for the rate of change of the parameter φ with MCC thickness were not conserved between the two methods.

DISCUSSION

The data presented here permit us to assess the ability of electrical impedance spectroscopy to characterize the cell environment of MCCs. Results show good correlation of impedance measurements with culture growth and indicate sensitivity to increasing culture thickness and net membrane capacitance. In addition, the differences in impedance characteristics of the three cell lines studied here, manifested by the parameter φ_{EIS}, indicate the utility of impedance spectroscopy as a method of comparison of in vitro tissue structure. Plots of the parameter for extracellular resistance,

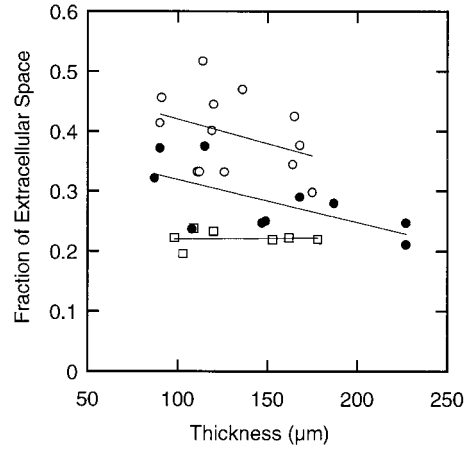

FIGURE 7 Extracellular space as a function of MCC thickness determined via a series of equilibrium C^{14}-inulin measurements using SiHa □, V79 ○, and V79/DOX ● MCCs.

R_e, as a function of culture thickness show that impedance measurements can be used to determine culture thickness and monitor growth. Such measurements can be done quickly and nondestructively. The net cell membrane capacitance, related to the parameter Y_o, is seen to change with culture thickness. Y_o shows a downward trend with increasing culture thickness, consistent with what is expected to occur if the cells behave according to the simple electrical model of Fig. 1 *b*.

The C^{14}-inulin measurements of extracellular space and the effect of tissue tortuosity on diffusion were consistent with previous studies done using spheroids (Casciari et al., 1988, Freyer and Sutherland, 1983) that compared a range of cell lines. In those studies there was no direct correlation between rates of diffusion for the two cell lines once the extracellular space had been accounted for, indicating that

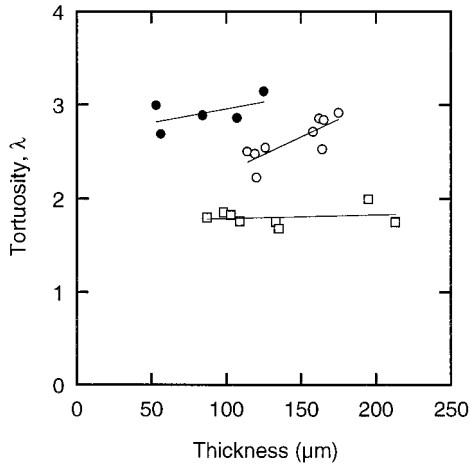

FIGURE 8 Estimate of the tortuosity factor, λ, within SiHa □, V79 ○, and V79/DOX ● MCCs. Results were obtained from analysis of C^{14}-inulin flux experiments. Each data point is from a separate experiment in which the rate of diffusion of C^{14}-inulin through the extracellular space of an MCC was used to determine an estimate of λ.

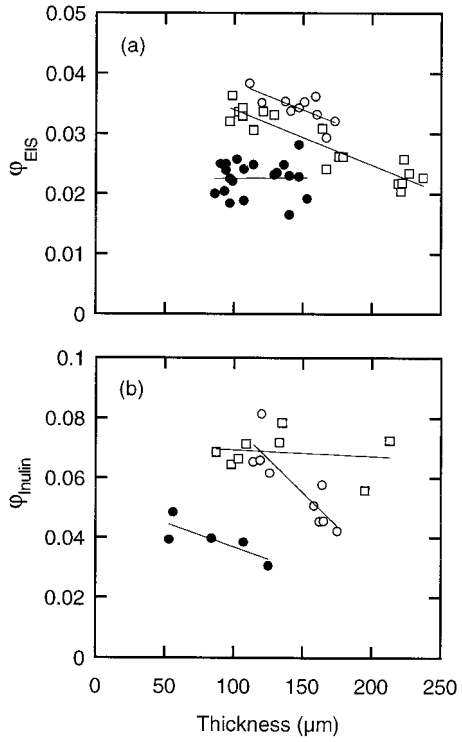

FIGURE 9 Comparison of the combined effect of tissue tortuosity and the fraction of extracellular space determined from electrical impedance and C^{14}-inulin diffusion measurements. (*a*) Results for calculation of φ_{EIS} from the data of Figs. 5 *a* and 6 *a* and Eq. 9. (*b*) Similar results for φ_{Inulin}, calculated using the data of Fig. 8 and Eq. 11. Data points show results for SiHa □, V79 ○, and V79/DOX ● MCCs.

the degree of extracellular tortuosity plays an important role in determining the barrier to diffusion posed by the culture. The general trend of decreasing extracellular space with increasing MCC thickness observed for both V79 and V79/DOX MCCs was not seen in the earlier spheroid study (Freyer and Sutherland, 1983). The possibility that the decrease was caused by incomplete removal of surface liquid during the wicking process was rejected because the effect was not observed for the SiHa MCCs, which have the smallest amount of extracellular space and would therefore be most susceptible to such a measurement artifact.

The combined effect of tortuosity and extracellular fraction calculated from impedance measurements did not match exactly with the results determined via C^{14}-inulin experiments. Although the estimates of φ differed by roughly a factor of two between impedance and diffusion methods, the two methods' rank ordering of the three cell lines were reasonably similar. The increase in the penetrative barrier posed by V79/DOX relative to V79 MCCs, observed in both impedance and diffusion measurements, was consistent with reported data of wild-type versus drug-resistant EMT-6 cells grown as spheroids (Kobayashi et al., 1993). In the Kobayashi report, visual assessment of histological sections found that spheroids grown from the drug-resistant cells formed a more compact structure than the wild-type cells. There are many possible explanations for the disagreement between the absolute values of φ determined using the two methods. The impedance results were obtained using a measurement jig that did not produce a uniform field over the entire surface area of the MCC. This is not necessarily a problem when experimental results, such as the parameter R_e, are empirically compared with MCC thickness. However, it does pose a problem when the data were applied to Eqs. 6–9, which implicitly require a uniform electrical field. The discrepancy may also derive from the fact that the impedance measurements were based on the conductivity of salt ions such as Na^+, Cl^-, and K^+, which are all small molecules (M.W. <100), whereas the diffusion data were derived from measurements made using the large C^{14}-inulin molecule (M.W. ~5175). However, it is not clear why the much larger inulin molecule would experience less resistance to diffusion within the extracellular space of the MCCs than would the small ions. Despite this disparity between the two methods, the results do indicate that the simple impedance spectroscopy technique is reasonably successful at comparing the relative barriers to diffusion presented by the different cell types grown as MCCs. In addition, impedance measurements made before and after experiments using MCCs could serve as a toxicity assay to determine the effect of a drug on the integrity of the cultures and cell membranes.

In conclusion, the results presented here indicate that electrical impedance spectroscopy can be a useful tool to characterize and monitor the cell environment of MCCs. The impedance system presented here is simple and requires little developmental labor; a commercially available measurement jig was used for these experiments. In addition, there are numerous automated impedance measurement devices that could be used to monitor MCCs in real time.

The authors thank W. R. Wilson (Auckland) for thoughtful advice pertaining to this paper.

REFERENCES

Ackmann, J. J. 1993. Complex bioelectric impedance measurement system for the frequency range from 5 Hz to 1 MHz. *Ann. Biomed. Eng.* 21:135–146.

Bao, J. Z., C. C. Davis, and R. E. Schmukler. 1993. Impedance spectroscopy of human erythrocytes: system calibration and nonlinear modeling. *IEEE Trans. Biomed. Eng.* 40:364–378.

Casciari, J. J., S. V. Sotirchos, and R. M. Sutherland. 1988. Glucose diffusivity in multicellular tumor spheroids. *Cancer Res.* 48:3905–3909.

Cole, K. S., and R. H. Cole. 1941. Dispersion and absorption in dielectrics. I. Alternating current characteristics. *J. Chem. Phys.* 9:341–351.

Cowan, D. S. M., K. O. Hicks, and W. R. Wilson. 1996. Multicellular membranes as an in vitro model for extravascular diffusion in tumors. *Br. J. Cancer.* 74:S28–S31.

Crank, J. 1975. The Mathematics of Diffusion. Clarendon Press, Oxford.

Durand, R. E. 1980. Variable radiobiological responses of spheroids. *Radiat. Res.* 81:85–99.

Durand, R. E. 1981. Flow cytometry studies of intracellular adriamycin in multicell spheroids in vitro. *Cancer Res.* 41:3495–3498.

Durand, R. E., and P. L. Olive. 1992. Evaluation of bioreductive drugs in multicell spheroids. *Int. J. Radiat. Oncol. Biol. Phys.* 22:689–692.

Foster, K. R., and H. P. Schwan. 1989. Dielectric properties of tissues and biological materials: a critical review. *Crit. Rev. Biomed. Eng.* 17: 25–104.

Freyer, J. P., and R. M. Sutherland. 1983. Determination of diffusion constants for metabolites in multicell tumor spheroids. *Adv. Exp. Med. Biol.* 159:463–475.

Freyer, J. P., E. Tustanoff, A. J. Franko, and R. M. Sutherland. 1984. In situ oxygen consumption rates of cells in V-79 multicellular spheroids during growth. *J. Cell. Physiol.* 118:53–61.

Hicks, K. O., S. J. Ohms, P. L. van Zijl, W. A. Denny, P. J. Hunter, and W. R. Wilson. 1997. An experimental and mathematical model for the extravascular transport of a DNA intercalator in tumors. *Br. J. Cancer.* 76:894–903.

Jain, R. K. 1987. Transport of molecules in the tumor interstitium: a review. *Cancer Res.* 47:3039–3051.

Kerr, D. J., and S. B. Kaye. 1987. Aspects of cytotoxic drug penetration, with particular reference to anthracyclines. *Cancer Chemother. Pharmacol.* 19:1–5.

Kerr, D. J., T. E. Wheldon, A. M. Kerr, and S. B. Kaye. 1987. In vitro chemosensitivity testing using the multicellular tumor spheroid model. *Cancer Drug Delivery.* 4:63–73.

Kobayashi, H., S. Man, C. H. Graham, S. J. Kapitain, B. A. Teicher, and R. S. Kerbel. 1993. Acquired multicellular-mediated resistance to alkylating agents in cancer. *Proc. Natl. Acad. Sci. USA.* 90:3294–3298.

Kwok, T. T., and R. M. Sutherland. 1991. The influence of cell-cell contact on radiosensitivity of human squamous carcinoma cells. *Radiat. Res.* 126:52–57.

Kyle, A., and A. I. Minchinton. 1999. Measurement of delivery and metabolism of tirapazamine through tumor tissue using the multilayered cell culture model. *Cancer Chemother. Pharmacol.* 43:213–220.

McRae, D. A., M. A. Esrick, and S. C. Mueller. 1997. Non-invasive, in-vivo electrical impedance of EMT-6 tumors during hyperthermia: correlation with morphology and tumor-growth-delay. *Int. J. Hyperthermia.* 13:1–20.

Minchinton, A. I., K. R. Wendt, K. A. Clow, and K. H. Fryer. 1997. Multilayers of cells growing on a permeable support: an in vitro tumor model. *Acta Oncologica.* 36:13–16.

Mueller-Klieser, W. 1997. Three-dimensional cell cultures: from molecular mechanisms to clinical applications. *Am. J. Physiol.* 273:C1109–C1123.

Nederman, T., J. Carlsson, and M. Malmqvist. 1981. Penetration of substances into tumor tissue: a methodological study on cellular spheroids. *In Vitro.* 17:290–298.

Nicholson, C., and J. M. Phillips. 1981. Ion diffusion modified by tortuosity and volume fraction in the extracellular microenvironment of the rat cerebellum. *J. Physiol.* 321:225–257.

Olive, P. L., and R. E. Durand. 1994. Drug and radiation resistance in spheroids: cell contact and kinetics. *Cancer Metast. Rev.* 13:121–138.

Pethig, R. 1979. Dielectric and Electronic Properties of Biological Materials. John Wiley and Sons, New York.

Press, W. H. 1992. Numerical Recipes in C: The Art of Scientific Computing. Cambridge University Press, Cambridge.

Rigaud, B., J. P. Morucci, and N. Chauveau. 1996. Bioelectrical impedance techniques in medicine. Part I: Bioimpedance measurement. Second section: impedance spectrometry. *Crit. Rev. Biomed. Eng.* 24:257–351.

Schwan, H. P. 1963. Determination of biological impedances. *In* Physical Techniques in Biological Research. Academic Press, New York. 323–406.

Sutherland, R. M. 1988. Cell and environment interactions in tumor microregions: the multicell spheroid model. *Science.* 240:177–184.